*Supporting Information for* **ja-2011-056852***:*

# Kinetic Effects Of Increased Proton Transfer Distance On Proton-Coupled Oxidations Of Phenol-Amines

Todd F. Markle, Ian J. Rhile, and James M. Mayer

Department of Chemistry, Box 351700, University of Washington, Seattle, WA 98195-1700

mayer@chem.washington.edu

**I. Complete citation for reference 64.**
M. J. Frisch, G. W. Trucks, H. B. Schlegel, G. E. Scuseria, M. A. Robb, J. R. Cheeseman, J. A. Montgomery, Jr., T. Vreven, K. N. Kudin, J. C. Burant, J. M. Millam, S. S. Iyengar, J. Tomasi, V. Barone, B. Mennucci, M. Cossi, G. Scalmani, N. Rega, G. A. Petersson, H. Nakatsuji, M. Hada, M. Ehara, K. Toyota, R. Fukuda, J. Hasegawa, M. Ishida, T. Nakajima, Y. Honda, O. Kitao, H. Nakai, M. Klene, X. Li, J. E. Knox, H. P. Hratchian, J. B. Cross, V. Bakken, C. Adamo, J. Jaramillo, R. Gomperts, R. E. Stratmann, O. Yazyev, A. J. Austin, R. Cammi, C. Pomelli, J. W. Ochterski, P. Y. Ayala, K. Morokuma, G. A. Voth, P. Salvador, J. J. Dannenberg, V. G. Zakrzewski, S. Dapprich, A. D. Daniels, M. C. Strain, O. Farkas, D. K. Malick, A. D. Rabuck, K. Raghavachari, J. B. Foresman, J. V. Ortiz, Q. Cui, A. G. Baboul, S. Clifford, J. Cioslowski, B. B. Stefanov, G. Liu, A. Liashenko, P. Piskorz, I. Komaromi, R. L. Martin, D. J. Fox, T. Keith, M. A. Al-Laham, C. Y. Peng, A. Nanayakkara, M. Challacombe, P. M. W. Gill, B. Johnson, W. Chen, M. W. Wong, C. Gonzalez, and J. A. Pople, Gaussian 03, Revision D.02, Gaussian, Inc., Wallingford CT, 2004.

## II. EXSY spectrum of compound 2.

Simple analysis of the EXSY spectrum, Figure S1, gives a rough estimate of the rate constant for the exchange process of 0.6 s$^{-1}$. This was determined using the relation: $k = t_m^{-1} \ln(r + 1 / r - 1)$, where $t_m$ is the mixing time and the term $r$ is related the intensity of the cross and diagonal peaks ($I_{AB}$, $I_{AA}$, and $I_{BB}$), $r = 4X_A X_B (I_{AA} + I_{BB})/2I_{AB} - (X_A - X_B)^2$, where $X$ is the mole fraction population of a given site.[1]
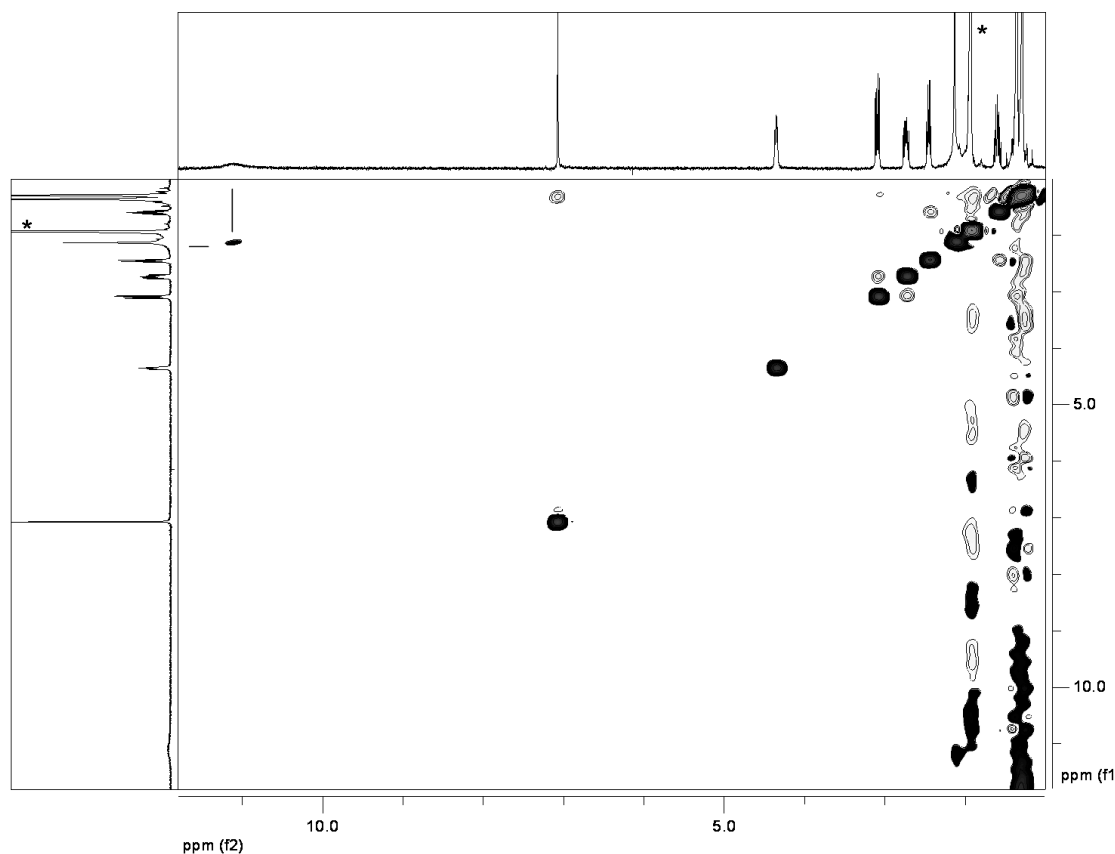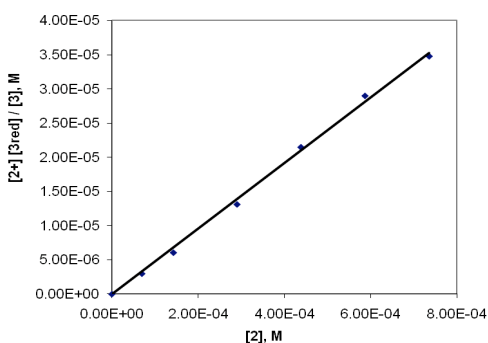


**Figure S1.** 2D EXSY $^1$H NMR spectrum of **2** (6 mM) in CD$_3$CN, collected at 298 K. The lines on the 2D spectrum indicate the exchange cross peak for the phenolic and amino protons. The asterisks on the 1D spectra indicate the residual solvent peak.

---

[1] Perrin, C. L.; Dwyer, T. J. *Chem. Rev.* **1990**, *90*, 935-967.

### III. Spectrophotometric determination of $K_{eq}$.

The equilibrium constant for reaction 2, $K_2$, was determined from the change in the position of the equilibrium with varying amounts of excess phenol. With known initial concentrations of the four species and the assumption of mass balance, the decrease in absorbance at $\lambda_{max}$ of **3a** (718 nm) was used to calculate equilibrium concentrations of **2**, **3a**, **2⁺**, and **3a⁰**. Plotting $[\mathbf{2^+}]_{eq}[\mathbf{3^0}]_{eq}/[\mathbf{3}]_{eq}$ vs. $[\mathbf{2}]_{eq}$ yields a straight line with a slope equal to $K_2$, here 0.049(8), $R^2 = 0.998$, Figure S2a. This treatment was repeated at various temperatures, giving the Van't Hoff plot, Figure S2.

a)                                                          b)



**Figure S2.** (a) Determination of $K_2$ at 295 K, see text. (b) Variation of $K_{eq}$ with temperature for the reaction of **3a** with **2** (filled circles) and $d_3$-**2** (open circles). Lines are fits to the Van't Hoff equation.

## IV. Solution IR spectra.

Compound **1** was deuterated via exchange with MeOD. IR spectra for **1** and $d_3$-**1** were collected in $CHCl_3$ solution, Figure S3. Upon deuteration, the broad band assigned to $\nu$OH, which overlaps with the sharper CH stretches at ca. 2800-3000 cm$^{-1}$, decreased and a new broad band centered at 2200 cm$^{-1}$, corresponding to the $\nu$OD stretch, appeared.



**Figure S3.** IR spectra of **1** (blue) and $d_3$-**1** (red).

## V. Crystallography.

**Table S1.** Collection and refinement data for the crystallographic structure of **2**.

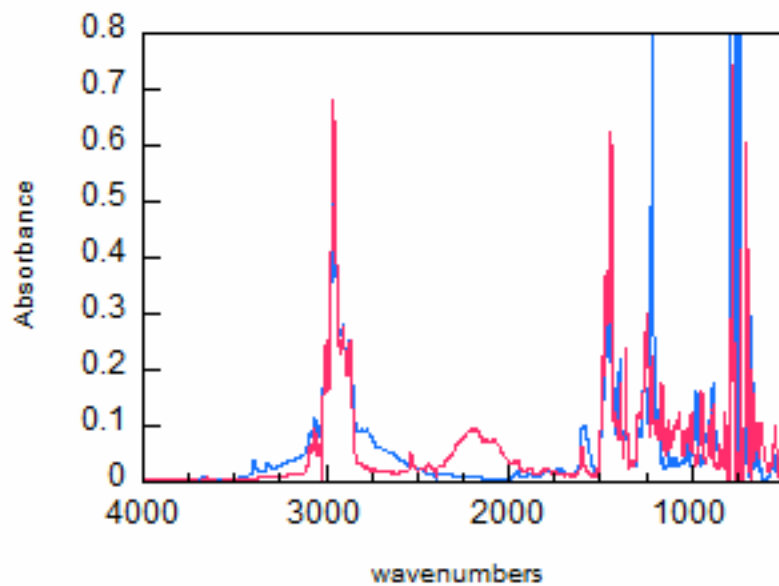| | |
|---|---|
| Empirical formula | $C_{17}H_{27}NO$ |
| Formula weight | 261.40 |
| Temperature | 208(2) K |
| Wavelength | 0.71073 Å |
| Crystal system | Orthorhombic |
| Space group | *Pbca* |
| Unit cell dimensions | $a = 9.5490(17)$ Å      $\alpha = 90°$. |
| | $b = 12.040(2)$ Å      $\beta = 90°$. |
| | $c = 27.566(5)$ Å      $\gamma = 90°$. |
| Volume | 3169.4(10) Å$^3$ |
| Z | 8 |
| Density (calculated) | 1.096 Mg/m$^3$ |
| Absorption coefficient | 0.067 mm$^{-1}$ |
| F(000) | 1152 |
| Crystal size | $0.12 \times 0.10 \times 0.04$ mm$^3$ |
| Crystal color/habit | colorless block |
| Theta range for data collection | 2.59 to 25.02°. |
| Index ranges | $-11 \leq h \leq 10, -11 \leq k \leq 14, -32 \leq l \leq 31$ |
| Reflections collected | 19339 |
| Independent reflections | 2794 [$R_{int} = 0.1033$] |
| Completeness to theta = 25.00° | 99.7% |
| Absorption correction | Semi-empirical from equivalents |
| Max. and min. transmission | 0.9973 and 0.9920 |
| Refinement method | Full-matrix least-squares on F$^2$ |
| Data / restraints / parameters | 2794 / 0 / 182 |
| Goodness-of-fit on F$^2$ | 1.060 |
| Final R indices [I>2sigma(I)] | $R_1 = 0.0698, wR_2 = 0.1420$ |
| *R* indices (all data) | $R_1 = 0.1381, wR_2 = 0.1660$ |
| Largest diff. peak and hole | 0.339 and $-0.206$ *e* Å$^{-3}$ |

## VI. DFT calculated geometries.

**Table S2.** B3LYP/6-31G(d,p) hydrogen bond geometries for **1** and **2**. Bond lengths are in Å, angles are in degrees.

|            | $d_{ON}$ | $d_{OH}$ | $d_{NH}$ | $\angle OHN$ | $r_0$ [a] |
|------------|----------|----------|----------|--------------|-----------|
| **1**      | 2.643    | 0.995    | 1.743    | 148.0        | 0.684     |
| **1$^{+\bullet}$** | 2.533 | 1.549 | 1.083 | 147.9        |           |
| **2**      | 2.808    | 0.985    | 1.934    | 146.4        | 0.897     |
| **2$^{+\bullet}$** | 2.646 | 1.699 | 1.072 | 145.9        |           |

[a] Proton transfer distance calculated following: Johannissen, L. O.; Irebo, T.; Sjödin, M.; Johansson, O.; Hammarström, L. *J. Phys. Chem. B.*, **2009**, *113*, 16214-16225.

**Table S3.** Effect of basis set and functional on the difference in $d_{ON}$ calculated for **1** and **2**.

|        | 6-311G(d) | 6-311++G(d,p) | 6-311++G(3d,3p) | cc-pVTZ | aug-cc-pVTZ |
|--------|-----------|---------------|-----------------|---------|-------------|
| BP86   | 0.148     | 0.171         | 0.171           | 0.162   | 0.169       |
| PBEPBE | 0.148     | 0.173         | 0.172           | 0.162   | 0.171       |
| B3LYP  | 0.156     | 0.178         | 0.179           | 0.171   | 0.180       |
| M06    | 0.149     | 0.165         | 0.168           | 0.161   | 0.168       |
| M062X  | 0.155     | 0.173         | 0.179           | 0.176   | 0.182       |

B3LYP/6-31G(d,p): $d_{ON}$ = 0.165 Å (gas phase),   0.163 Å (with PCM model of MeCN solvent)

**Table S4.** Calculated $d_{ON}$, $d_{OH}$, $d_{NH}$, and $\angle OHN$ values for **1**.

|        | 6-311G(d) | 6-311++G(d,p) | 6-311++G(3d,3p) | cc-pVTZ | aug-cc-pVTZ |
|--------|-----------|---------------|-----------------|---------|-------------|
|        |           |               | $d_{ON}$        |         |             |
| BP86   | 2.626     | 2.631         | 2.629           | 2.630   | 2.629       |
| PBEPBE | 2.623     | 2.628         | 2.626           | 2.627   | 2.626       |
| B3LYP  | 2.650     | 2.657         | 2.655           | 2.655   | 2.655       |
| M06    | 2.655     | 2.667         | 2.670           | 2.670   | 2.670       |
| M062X  | 2.660     | 2.669         | 2.667           | 2.662   | 2.664       |
|        |           |               | $d_{OH}$        |         |             |
| BP86   | 1.013     | 1.011         | 1.010           | 1.010   | 1.010       |
| PBEPBE | 1.011     | 1.009         | 1.008           | 1.009   | 1.009       |
| B3LYP  | 0.989     | 0.988         | 0.987           | 0.988   | 0.987       |
| M06    | 0.985     | 0.983         | 0.981           | 0.981   | 0.981       |
| M062X  | 0.983     | 0.982         | 0.982           | 0.984   | 0.983       |
|        |           |               | $d_{NH}$        |         |             |
| BP86   | 1.708     | 1.711         | 1.708           | 1.708   | 1.708       |
| PBEPBE | 1.707     | 1.710         | 1.706           | 1.706   | 1.706       |
| B3LYP  | 1.769     | 1.774         | 1.771           | 1.770   | 1.772       |

| | | | | | |
|---|---|---|---|---|---|
| M06 | 1.788 | 1.800 | 1.803 | 1.802 | 1.803 |
| M062X | 1.797 | 1.803 | 1.797 | 1.790 | 1.794 |
| | | | ∠OHN | | |
| BP86 | 148.6 | 149.2 | 149.6 | 149.6 | 149.5 |
| PBEPBE | 148.5 | 149.2 | 149.6 | 149.7 | 149.6 |
| B3LYP | 146.3 | 146.8 | 147.1 | 147.2 | 147.0 |
| M06 | 145.0 | 145.3 | 145.4 | 145.6 | 145.4 |
| M062X | 144.7 | 145.3 | 145.8 | 145.9 | 145.8 |

**Table S5.** Calculated $d_{ON}$, $d_{OH}$, $d_{NH}$, and ∠OHN values for **2**.

| | 6-311G(d) | 6-311++G(d,p) | 6-311++G(3d,3p) | cc-pVTZ | aug-cc-pVTZ |
|---|---|---|---|---|---|
| | | | $d_{ON}$ | | |
| BP86 | 2.774 | 2.801 | 2.799 | 2.792 | 2.798 |
| PBEPBE | 2.772 | 2.801 | 2.798 | 2.790 | 2.797 |
| B3LYP | 2.806 | 2.835 | 2.834 | 2.826 | 2.835 |
| M06 | 2.804 | 2.832 | 2.837 | 2.831 | 2.837 |
| M062X | 2.816 | 2.843 | 2.846 | 2.838 | 2.846 |
| | | | $d_{OH}$ | | |
| BP86 | 1.002 | 0.998 | 0.997 | 0.998 | 0.998 |
| PBEPBE | 1.000 | 0.996 | 0.995 | 0.997 | 0.996 |
| B3LYP | 0.982 | 0.980 | 0.978 | 0.979 | 0.979 |
| M06 | 0.980 | 0.977 | 0.975 | 0.976 | 0.975 |
| M062X | 0.976 | 0.974 | 0.973 | 0.974 | 0.974 |
| | | | $d_{NH}$ | | |
| BP86 | 1.876 | 1.908 | 1.904 | 1.893 | 1.902 |
| PBEPBE | 1.876 | 1.910 | 1.905 | 1.892 | 1.903 |
| B3LYP | 1.942 | 1.975 | 1.973 | 1.961 | 1.974 |
| M06 | 1.951 | 1.983 | 1.989 | 1.981 | 1.990 |
| M062X | 1.970 | 1.999 | 2.001 | 1.991 | 2.002 |
| | | | ∠OHN | | |
| BP86 | 147.5 | 147.5 | 148.0 | 148.3 | 148.0 |
| PBEPBE | 147.4 | 147.4 | 147.9 | 148.3 | 147.9 |
| B3LYP | 145.4 | 145.2 | 145.5 | 145.8 | 145.4 |
| M06 | 144.1 | 143.9 | 144.1 | 144.4 | 144.0 |
| M062X | 143.6 | 143.6 | 143.9 | 144.1 | 143.7 |

## VII. Oxidations using iron(III)-*tris*-diimine oxidants.



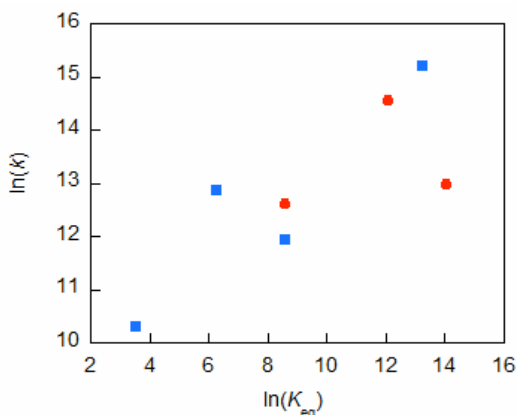**Figure S4.**    Variation of rate constants $\ln(k)$ with $\ln(K_{eq})$ for the reactions of $[Fe(N-N)_3]^{3+}$ with **1** (■)[2] and **2** (●).

   While the CPET mechanism is generally indicated for all the reactions described in this report, the thermodynamic arguments are not as strong for the reactions of the iron tris-diimine oxidants,   which have higher apparent barriers and lower $\Delta G°_{ET}$.   For example, the $k = (4.3 \pm 0.4) \times 10^5$ M$^{-1}$ s$^{-1}$ for **2** + $[Fe(5,5\text{ -Me}_2bpy)_3]^{3+}$ corresponds to an Eyring barrier ($\Delta G^{\ddagger}$) of 0.42 eV, which is lower than the estimated $\Delta G°_{ET} \cong -0.51$ V but still within the uncertainty of this estimate.  Still, a CPET pathway is most consistent with the results, such as the primary KIE of $2.6 \pm 0.4$ for **1** + $[Fe(5,5\text{ -Me}_2bpy)_3]^{3+}$.[2]   In addition, the rate constants for the reactions of **2** follow the trends expected from Marcus cross-relation.  For instance, the reaction of **2** + $[Fe(Me_4phen)_3]^{3+}$ is *ca.* 5 times slower than the reaction of **2** + **3d⁺** due to a slightly higher driving force (0.02 V) and the higher intrinsic barriers for $[Fe(N-N)_3]^{3+}$ *vs.* the amminium reagents.[3]  Thus all of the reactions studied here are indicated to proceed by CPET.

[2]  Rhile, I. J.; Markle, T. F.; Nagao, H.; DiPasquale, A. G.; Lam, O. P.; Lockwood, M. A.; Rotter, K.; Mayer, J. M. *J. Am. Chem. Soc.* **2006**, *128*, 6075-6088.

[3]   A factor of nine is predicted from the Marcus cross relation, $k_{2+ox} = (k_{se,ox}\, k_{se,\mathbf{2}}\, K_{eq}\, f)^{1/2}$ using the rates for the self-exchange reactions in MeCN ($k_{se,ox}$):  $6.9 \times 10^8$ M$^{-1}$ s$^{-1}$ for **3c⁺/⁰** and $1.7 \times 10^7$ M$^{-1}$ s$^{-1}$ for $[Fe(Me_4phen)_3]^{3+/2+}$.  (a) Eberson, L. *Electron Transfer Reactions in Organic Chemistry*; Springer-Verlag: New York, 1987; p. 51.   (b) Wherland, S. *Coord. Chem. Rev.* **1993**, *123*, 169-199.